Nuclear Inst. and Methods in Physics Research, A 921 (2019) 18–21

Contents lists available at ScienceDirect

Nuclear Inst. and Methods in Physics Research, A

journal homepage: www.elsevier.com/locate/nima

Effect of CsI(Tl) micro-conical-frustums on the performance of the pixelated CsI(Tl) scintillation screen in X-ray imaging

Hui Chen, Mu Gu *, Xiaolin Liu, Juannan Zhang, Shiming Huang, Bo Liu, Chen Ni

Shanghai Key Laboratory of Special Artificial Microstructure Materials and Technology, School of Physics Science and Engineering, Tongji University, Shanghai 200092, PR China

ARTICLE INFO

Keywords:
Pixelated CsI(Tl) scintillation screen
Oxidized silicon micro-pore array template
Shape of CsI(Tl) micro-conical-frustum
Performance in X-ray imaging

ABSTRACT

The pixelated CsI(Tl) scintillation screen based on oxidized silicon micro-pore array template with CsI(Tl) micro-conical-frustums (CMCF) was proposed. The effect of the CMCF on the performance of the pixelated CsI(Tl) scintillation screen in X-ray imaging was studied by using Geant4 Monte Carlo simulation code. The variations of the light output (LO), modulation transfer function (MTF) and detective quantum efficiency (DQE) for the screen with the cone angle β of the CMCF in X-ray imaging were revealed. The results show that the LO of the pixelated scintillation screen with CMCF is superior to that of the screens with CsI(Tl) micro-cylinders (CMC) or with reversed CsI(Tl) micro-conical-frustums (RCMCF), but the spatial resolution of the X-ray imaging system by using the pixelated scintillation screen with RCMCF is better than that by using the screens with CMCF or with CMC. At low frequency, the cone angle β corresponding to DQEs from good to bad are 2.40°, 0.00° and -2.40°. But at high frequency, the cone angle β corresponding to DQEs from good to bad change to 2.40°, -2.40° and 0.00°. The reason is that, for a pixelated scintillation screen, the DQE for the screen not only depends on the efficiency of X-ray absorption, but also depends on the number of scintillation photons exiting the bottom the screen per interacting X-ray photon and its Poisson excess, and MTF. The simulated results of DQEs show that the comprehensive performance of the pixelated CsI(Tl) screen with CMCF in X-ray imaging is better than that of the screens with CMC or with CRMCF.

1. Introduction

CsI(Tl) scintillation screen has be widely used in X-ray imaging, such as nuclear medical imaging, non-destructive testing, etc. because of its high scintillation efficiency and good spectral matching with many silicon-based optical imaging detectors [1–4]. To ensure adequate detection efficiency, the scintillation screen usually requires a sufficient thickness. However, due to the lateral spreading of the scintillation light, increasing the thickness of the scintillation screen typically comes at the expense of its spatial resolution [2]. To overcome this limitation, the CsI(Tl) scintillation screen with needle-like columnar structure was developed by a thermal evaporation method [3]. The vertical columnar structure can suppress the lateral spreading of scintillation light and preserve the spatial resolution of X-ray imaging. However, this kind of structure is not perfect. The cross-talk of scintillation light between the adjacent columns still exists due to the lack of effective optical isolation, especially for hard X-ray imaging. In order to solve this problem, the pixelated CsI(Tl) scintillation screens composed of oxidized silicon micro-pore array templates filled with CsI(Tl) scintillator have been developed [5–9]. The scintillation light with an incident angle less than the critical angle α_c of total internal reflection will be led propagating along the CsI(Tl) micro-columns, and the light entering the pore walls will almost be absorbed and difficult to transmit to adjacent columns [5,6]. It has been reported that the period of the CsI(Tl) micro-column array of the screen that can be used in X-ray imaging up to now can reach to 4 μm with the column height ranged from 40 μm to 100 μm, and the spatial resolution of the X-ray imaging system with the screen exceeds 100 lp/mm [10,11]. In order to avoid the crosstalk between adjacent CsI(Tl) micro-columns, a certain thickness of silicon wall, such as ~1 μm, should be maintained. Although the spatial resolution of X-ray imaging will increase with the decrease of the period of the CsI(Tl) micro-column array, the filling rate of CsI(Tl) scintillator in the pixelated screen will be reduced, which will reduce the light output (LO) of the screen in X-ray imaging. Therefore, it is of great significance to study how to improve the LO under a small micro-pore array period of the pixelated CsI(Tl) scintillation screen.

The refractive index of the SiO_2 layers covering on the surface of the pore walls of the oxidized silicon micro-pore array is 1.46 and that of CsI(Tl) is 1.74, so the critical angle α_c of total internal reflection is 33.0°. The common micro-columns of the pixelated CsI(Tl) scintillation screen available are cylindrical in shape [11] because they seem to have

* Corresponding author.
E-mail address: mgu@tongji.edu.cn (M. Gu).

https://doi.org/10.1016/j.nima.2018.12.006
Received 21 August 2018; Received in revised form 18 November 2018; Accepted 3 December 2018
Available online 6 December 2018

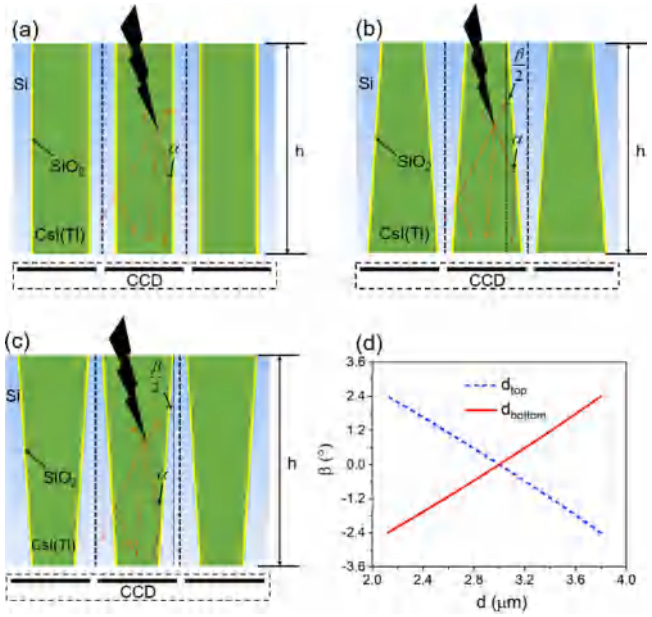

Fig. 1. The schematic diagram of the pixelated CsI(Tl) scintillation screens based on oxidized silicon micro-pore array templates with (a) CsI(Tl) micro-cylinder, (b) CsI(Tl) micro-conical-frustum, (c) reversed CsI(Tl) micro-conical-frustum; (d) The cone angle β of the CsI(Tl) micro-conical-frustum as a function of its top or bottom diameter.

a better light guiding effect than square or hexagonal micro-columns. The scintillation light with an incident angle less than the guiding cone angle $\theta = 2\alpha_c$ can propagate along the columns. It has been reported that micro-conical-frustum pores can be prepared in silicon wafers by metal-assisted chemical etching [12,13]. A micro-conical-frustum can have a larger guiding cone angle than a micro-cylinder. If the micro-pores in a silicon micro-pore array template can be made into micro-conical-frustums, it will be helpful to improve the LO of the pixelated scintillation screen. Therefore, it is necessary to propose a pixelated CsI(Tl) scintillation screen based on oxidized silicon micro-pore array template with CsI(Tl) micro-conical-frustums (CMCF) and predict the performance of the screen in X-ray imaging with the shape of the CMCF through theoretical simulation.

2. Materials and methods

2.1. Screen structures

The pixelated CsI(Tl) scintillation screens were composed of oxidized silicon micro-pore array templates filled with CsI(Tl) scintillator. The CsI(Tl) micro-columns in the screen for comparison were cylindrical with a diameter $d_c = 3.0$ μm and a height $h = 40.0$ μm arranged in a square array with a period of 4.0 μm. The micro-columns were separated by 0.8 μm thick silicon walls covered with 0.1 μm thick SiO_2 layers at each side, as shown in Fig. 1(a). The CMCF in different shapes in the pixelated CsI(Tl) scintillation screens for simulation are shown in Fig. 1(b) and 1(c). The top of the screens face the X-ray source and the bottom of the screens face the ideal charge coupled devices (CCDs). The optical coupling agent between the scintillation screens and CCDs is silicon oil with refractive index $n = 1.43$.

In order to study the effect of CMCF on X-ray imaging performance of the pixelated CsI(Tl) scintillation screen, the height, volume and arrangement of the CMCF were set to be the same as that of the CsI(Tl) micro-cylinder (CMC) mentioned above. If the top and bottom diameters of the CMCF are represented by d_{top} and d_{bottom}, the cone angle β of the CMCF can be expressed as

$$\beta = 2\arctan\frac{(d_{bottom} - d_{top})}{2h} \quad (1)$$

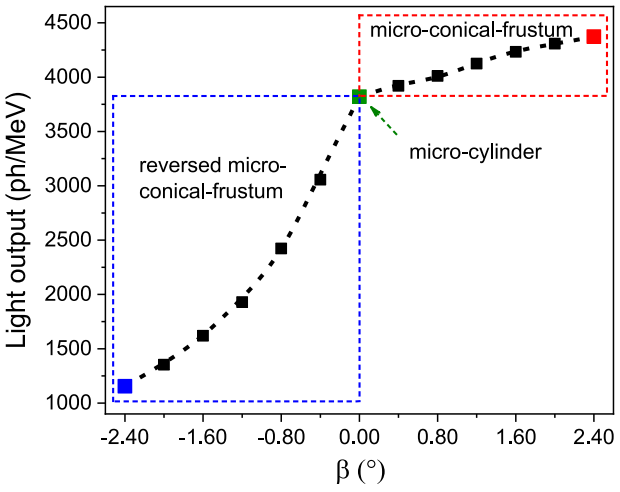

Fig. 2. The LO of the pixelated CsI(Tl) scintillation screen as a function of the cone angle β.

and the relation among d_{top}, d_{bottom} and d_c can be expressed as

$$\frac{1}{3}\left(d_{top}^2 + d_{top}d_{bottom} + d_{bottom}^2\right) = d_c^2. \quad (2)$$

The cone angle β of the CMCF as a function of its top or bottom diameter is shown in Fig. 1(d). When d_{top} or d_{bottom} reaches a maximum of 3.8 μm, the cone angle β equals −2.40° or 2.40°, respectively.

2.2. Simulation process

The effect of CMCF on the performance of the pixelated CsI(Tl) scintillation screen in X-ray imaging were characterized by the variations of the light output (LO), modulation transfer function (MTF) and detective quantum efficiency (DQE) with the cone angle β. When a scintillation screen is irradiated by X-rays, the scintillation light will be generated in the screen. Part of the scintillation light will be emitted from the bottom of the screen. The LO of the scintillation screen in this work was defined as the number of scintillation photons emitted from the bottom of the scintillation screen under X-ray irradiation per unit energy. The spatial resolution of an X-ray imaging system is commonly described by its MTF. In this work, the MTFs were simulated according to the standard edge measurement method [14]. The values of MTFs at zero spatial frequency were normalized to unit. The spatial resolutions of the systems with the pixelated CsI(Tl) scintillation screens having different cone angle β of the CMCF were defined by the spatial frequencies where MTFs = 0.1. The DQE is used to characterize an X-ray imaging detector by indicating how much the signal-to-noise ratio of the input image deteriorates during the detection process. In this work, the DQEs of the detectors with the pixelated CsI(Tl) scintillation screens having different cone angle β of the CMCF were simulated by using the Fujita–Lubberts–Swank (FLS) method [15–17].

The Monte Carlo simulation was carried out by using version 10.0 of Geant4 Monte Carlo simulation code [18,19]. The light yield, emission spectrum, optical attenuation coefficient and refractive index of CsI(Tl) scintillator used for simulation were obtained from Refs. [20–23]. And the refractive indices, optical attenuation coefficients of Si and SiO_2 were obtained from Refs. [22,24,25]. The energy of the parallel incident X-ray was set to 15 keV. The reliability of the simulating process can be verified by the simulated results of our other work [26] on CsI(Tl) scintillation screen proved by experiment [8].

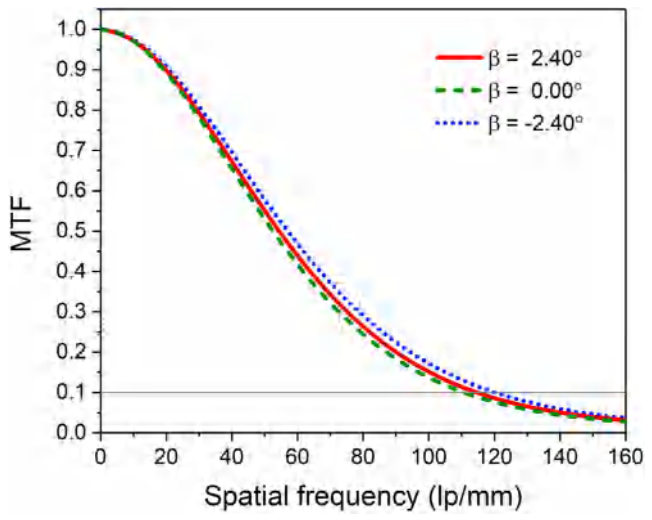

Fig. 3. The MTFs of the X-ray imaging systems by using the pixelated CsI(Tl) scintillation screens with the cone angle β of the micro-conical-frustums at 2.40°, 0.00° and −2.40°.

3. Results and discussion

3.1. Light output

The LO of the pixelated CsI(Tl) scintillation screen as a function of the cone angle β of the CMCF is shown in Fig. 2. It can be seen that the LO increases with the increase of the cone angle β because the guiding cone angle $\theta = 2\alpha_c + \beta$. When β is −2.40°, 0.00° and 2.40°, the LO equals 1154 ph/MeV, 3820 ph/MeV and 4308 ph/MeV, respectively. This means that the LO of the screen with β at −2.40° is only 30.2% of that with β at 0.00°, and the LO of the screen with β at 2.40° can reach 114.5% of that with β at 0.00°.

3.2. Modulation transfer function

The MTFs of the X-ray imaging systems by using the pixelated CsI(Tl) screens with the cone angle β of the CMCF at 2.40°, 0.00° and −2.40° are illustrated in Fig. 3. It can be seen that the MTF when $\beta = -2.40°$ is slightly better than that when $\beta = 2.40°$, and the MTF when $\beta = 2.40°$ is slightly better than that when $\beta = 0.00°$. Overall, however, there are not much differences among the three MTFs because they are mainly determined by the period of the CMCF array. The spatial resolutions in terms of MTFs for the pixelated CsI(Tl) screens with β at 2.40°, 0.00° and −2.40° are 115 lp/mm, 111 lp/mm and 120 lp/mm, respectively. The spatial resolution for β at 2.40° is about 3.4% higher than that for β at 0.00° because the CMCF has a better light guiding effect than that of the CMC, and the spatial resolution for β at −2.40° is about 8.5% higher than that for β at 0.00° because the reversed CsI(Tl) micro-conical-frustum (RCMCF) is superior to CMC in eliminating the scintillation light spreads laterally before reaching the bottom of the scintillation screen.

3.3. Detective quantum efficiency

The DQE at zero spatial frequency, i.e. DQE(0), of the X-ray imaging detector by using the pixelated CsI(Tl) screen as a function of the cone angle β of the CsI(Tl) micro-conical-frustum is shown in Fig. 4(a). It can be seen that the DQE(0) increases with the increase of the cone angle β, although the efficiencies of the X-ray absorption of the screens with different cone angle β are basically equal because the height, volume and arrangement of the CMCF were set to be the same. The reason is that, for a pixelated scintillation screen, the DQE(0) for the screen not only depends on the efficiency of X-ray absorption, but also depends on the number of scintillation photons exiting the bottom the screen per interacting X-ray photon and its Poisson excess as defined in Ref. [27]. The DQE(0) for the pixelated screen with CMCF is better than that with CMC, and the DQE(0) for the pixelated screen with CMC is better than that with RCMCF. When β is 2.40°, 0.00° and −2.40°, the DQE(0) is 0.270, 0.248 and 0.217, respectively. That is, the DQE(0) when $\beta = 2.40°$ can reach 108.9% of that when $\beta = 0.00°$, and the DQE(0) when $\beta = -2.40°$ is only 87.5% of that when $\beta = 0.00°$.

The DQEs of the X-ray imaging detectors by using the pixelated CsI(Tl) screens with the cone angle β of the CMCF at 2.40°, 0.00° and −2.40° as a function of spatial frequency are shown in Fig. 4(b). It can be seen that all DQEs decrease with the increase of spatial frequency because when MTFs are small, they are proportional to the square of the MTFs. At low frequency, the cone angle β corresponding to DQEs from good to bad are 2.40°, 0.00° and −2.40°. But at high frequency, the cone angle β corresponding to DQEs from good to bad change to 2.40°, −2.40° and 0.00°. The crossover of the DQEs when $\beta = 0.00°$ and −2.40° occurs at the spatial frequency about 51 lp/mm. The reason is that although the LO of the pixelated CsI(Tl) screen with RCMCF is not as good as that of the screen with CMC, the MTF by using the former screen is better than that by using the latter screen. Combined with the above results, it can be seen that the DQE for the pixelated CsI(Tl) screen with CMCF in X-ray imaging is better than that with CMC or with RCMCF at all frequencies. This means the former screen has the best comprehensive performance in X-ray imaging.

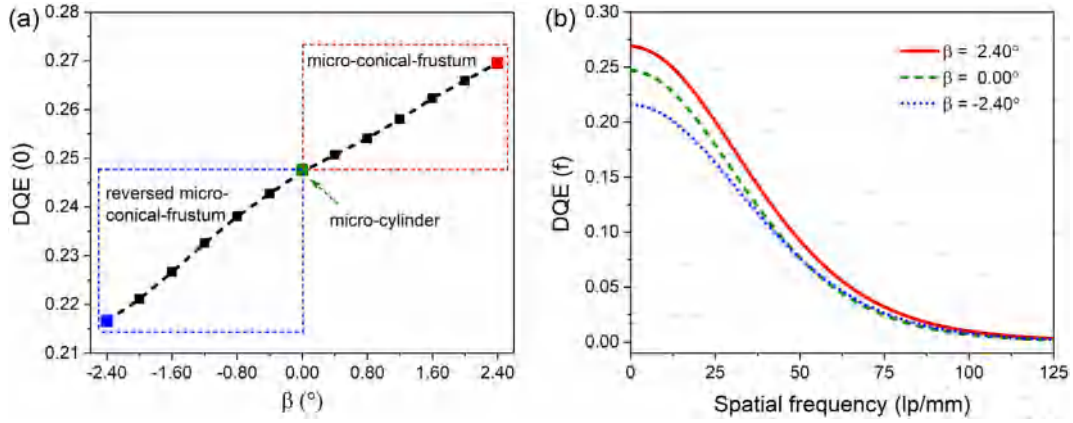

Fig. 4. (a) The DQE(0) of the X-ray imaging detector by using the pixelated CsI(Tl) screen as a function of the cone angle β of the micro-conical-frustum. (b) The DQEs of the X-ray imaging detectors by using the pixelated CsI(Tl) screens with the cone angle β of the micro-conical-frustums at 2.40°, 0.00° and −2.40° as a function of spatial frequency.

4. Conclusion

In conclusion, the performances of the pixelated CsI(Tl) screens based on oxidized silicon micro-pore array templates with different shapes of CMCF in X-ray imaging were investigated by using Geant4 Monte Carlo simulation code. The results show that the LO of the screen increases with the increase of the cone angle β of the CMCF. The LO of the screen with β at 2.40° can reach 114.5% of that with β at 0.00°, while the LO of the screen with β at −2.40° is only 30.2% of that with β at 0.00°. The MTF of the X-ray imaging system by using the pixelated CsI(Tl) screen with the cone angle β of CMCF at −2.40° is slightly better than that with β at 2.40°, and the MTF with β at 2.40° is slightly better than that with β at 0.00°. The spatial resolutions in terms of MTFs for the pixelated CsI(Tl) screens with β at 2.40°, 0.00° and -2.40° are 115 lp/mm, 111 lp/mm and 120 lp/mm, respectively. This means the spatial resolution by using the screen with RCMCF is better than that by using the screen with CMCF, and the spatial resolution by using the screen with CMCF is better than that by using the screen with CMC. At low spatial frequency, the cone angle β corresponding to the DQE of the X-ray imaging detector by using the pixelated CsI(Tl) screen with CMCF from good to bad are 2.40°, 0.00° and −2.40°. The reason is that, for a pixelated scintillation screen, the DQE(0) for the screen not only depends on the efficiency of X-ray absorption, but also depends on the number of scintillation photons exiting the bottom the screen per interacting X-ray photon and its Poisson excess. At high spatial frequency, the cone angle β corresponding to the DQE from good to bad change to 2.40°, −2.40° and 0.00°because the influence of MTF on DQE becomes important. Although the spatial resolution by using the screen with RCMCF is superior to that by using the screens with CMCF or with CMC, according to the results of DQEs, the comprehensive performance of X-ray imaging by using the pixelated CsI(Tl) scintillation screen with CMCF is the best. The quantitative results of this work can provide a useful guidance for optimization and fabrication of the pixelated CsI(Tl) scintillation screen.

Acknowledgment

This work is supported by National Natural Science Foundation of China (Grant Nos. 11675121, 11475128 and 11775160).

References

[1] M. Nikl, Scintillation detectors for X-rays, Meas. Sci. Technol. 17 (2006) R37–R54.
[2] T. Martin, A. Koch, Recent developments in X-ray imaging with micrometer spatial resolution, J. Synchrotron Radiat. 13 (2006) 180–194.
[3] D. Yao, M. Gu, X. Liu, S. Huang, B. Liu, C. Ni, Fabrication and performance of CsI(Tl) scintillation films with pixel-like columnar-matrix structure, IEEE Trans. Nucl. Sci. 62 (2015) 699–703.
[4] B. Zhao, X. Qin, Z. Feng, C. Wei, Y. Chen, B. Wang, L. Wei, Performance evaluation of CsI screens for X-ray imaging, Chinese Phys. C 38 (2014) 116003.
[5] P. Kleimann, J. Linnros, C. Fröjdh, C.S. Petersson, An X-ray imaging pixel detector based on scintillator filled pores in a silicon matrix, Nucl. Instrum. Methods Phys. Res. A 460 (2001) 15–19.
[6] X. Badel, B. Norlin, P. Kleimann, L. Williams, S.J. Moody, G.C. Tyrrell, C. Frojdh, J. Linnros, Performance of scintillating waveguides for CCD-based X-ray detectors, IEEE Trans. Nucl. Sci. 53 (2006) 3–8.
[7] M. Simon, K.J. Engel, B. Menser, X. Badel, J. Linnros, X-ray imaging performance of scintillator-filled silicon pore arrays, Med. Phys. 35 (2008) 968–981.
[8] O. Svenonius, A. Sahlholm, P. Wiklund, J. Linnros, Performance of an X-ray imaging detector based on a structured scintillator, Nucl. Instrum. Methods Phys. Res. A 607 (2009) 138–140.
[9] Y. Hormozan, S.H. Yun, O. Svenonius, J. Linnros, Towards high-resolution X-ray imaging using a structured scintillator, IEEE Trans. Nucl. Sci. 59 (2012) 19–23.
[10] Y. Hormozan, I. Sychugov, J. Linnros, High-resolution X-ray imaging using a structured scintillator, Med. Phys. 43 (2016) 696–701.
[11] S. Liu, M. Gu, H. Chen, Z. Sun, X. Liu, B. Liu, S. Huang, J. Zhang, Performance of pixelated CsI scintillation screen with hexagonal array arrangement prepared by vacuum melting injection method, Nucl. Instrum. Methods Phys. Res. A 903 (2018) 18–24.
[12] C. Lee, K. Tsujino, Y. Kanda, S. Ikeda, M. Matsumura, Pore formation in silicon by wet etching using micrometre-sized metal particles as catalysts, J. Mater. Chem. 18 (2008) 1015–1020.
[13] C. Chartier, S. Bastide, C. Lévy-Clément, Metal-assisted chemical etching of silicon in HF-H_2O_2, Electrochim. Acta 53 (2008) 5509–5516.
[14] E. Samei, M.J. Flynn, D.A. Reimann, A method for measuring the presampled MTF of digital radiographic systems using an edge test device, Med. Phys. 25 (1998) 102–113.
[15] J. Star-Lack, M. Sun, A. Meyer, D. Morf, D. Constantin, R. Fahrig, E. Abel, Rapid Monte Carlo simulation of detector DQE(f), Med. Phys. 41 (2014) 031916.
[16] J. Star-Lack, D. Shedlock, D. Swahn, D. Humber, A. Wang, H. Hirsh, G. Zentai, D. Sawkey, I. Kruger, M. Sun, E. Abel, G. Virshup, M. Shin, R. Fahrig, A piecewise-focused high DQE detector for MV imaging, Med. Phys. 42 (2015) 5084–5099.
[17] E. Abel, M. Sun, D. Constanin, R. Fahrig, J. Star-Lack, User-friendly, ultra-fast simulation of detector DQE(f), Proc. SPIE 8668 (2013) 86683O.
[18] S. Agostinelli, J. Allison, K. Amako, J. Apostolakis, et al., Geant-4a simulation toolkit, Nucl. Instrum. Methods Phys. Res. A 506 (2003) 250–303.
[19] J. Allison, K. Amako, J. Apostolakis, H. Araujo, et al., Geant4 developments and applications, IEEE Trans. Nucl. Sci. 53 (2006) 270–278.
[20] P. Lecoq, Development of new scintillators for medical applications, Nucl. Instrum. Methods Phys. Res. A 809 (2016) 130–139.
[21] H. Grassmann, E. Lorenz, H.G. Moser, Properties of CsI(Tl) - renaissance of an old scintillation material, Nucl. Instrum. Methods Phys. Res. A 228 (1985) 323–326.
[22] C.L. Woody, J.A. Kierstead, P.W. Levy, S. Stoll, Radiation damage in undoped CsI and CsI(Tl), IEEE Trans. Nucl. Sci. 39 (1992) 524–531.
[23] D. Smith, E. Shiles, M. Inokuti, E. Palik, Handbook of Optical Constants of Solids, Academic Press, 1985.
[24] D. Aspnes, A. Studna, Dielectric functions and optical parameters of Si, Ge, GaP, GaAs, GaSb, InP, InAs, and InSb from 1.5 to 60 eV, Phys. Rev. B 27 (1983) 985–1009.
[25] L. Gao, F. Lemarchand, M. Lequime, Refractive index determination of SiO_2 layer in the UV/Vis/NIR range: Spectrophotometric reverse engineering on single and bi-layer designs, J. Europ. Opt. Soc. Rap. Public. 8 (2013) 13010.
[26] H. Chen, M. Gu, X. Liu, S. Huang, B. Liu, J. Zhang, Spatial resolution and light output of pixelated CsI(Tl) scintillation screen based on oxidized silicon micropore array template, J. Instrum. 13 (2018) P07002.
[27] I.A. Cunningham, M.S. Westmore, A. Fenster, A spatial-frequency dependent quantum accounting diagram and detective quantum efficiency model of signal and noise propagation in cascaded imaging systems, Med. Phys. 21 (1994) 417–427.